enol-derived acid chloride to a carboxylate group. The carboxylate group forms a salt-bridge linkage to the protonated imidazole ring of histidine-57. This linkage precludes a water molecule from attacking the acyl linkage. Reactivation involves the reorientation of the terminal carboxylate group so that the salt bridge to histidine-57 is broken. The result is the rapid deacylation of the complex with the release of the isomerized (*E*)-4-benzyl-2-pentenedoic acid and native enzyme.

ACKNOWLEDGMENTS

We thank David R. Davies for a gift of γ-chymotrypsin crystals. We are grateful to Gregory A. Petsko for helpful discussions and for providing crystallographic facilities.

REFERENCES

Bernstein, F. C., Koetzle, T. F., Williams, G. J. B., Meyer, E. F., Jr., Brire, M. D., Rodgers, Y. R., Kenard, O., Shimanduchi, T., & Tasumi, M. (1977) *J. Mol. Biol. 112*, 535-542.

Cohen, G. H., Silverton, E. W., & Davies, D. R. (1981) *J. Mol. Biol. 148*, 449-479.

Gelb, M. H., & Abeles, R. H. (1984) *Biochemistry 23*, 6596-6604.

Henderson, R. (1970) *J. Mol. Biol. 54*, 341-354.

Hendrickson, W. A., & Konnert, J. H. (1980) in *Biomolecular Structure, Conformation, Function and Evolution* (Srinivason, R., Ed.) Vol. I, pp 43-57, Pergamon, New York.

Hummel, B. C. W. (1959) *Can. J. Biochem. Physiol. 37*, 1393-1399.

James, M. N. G., Sielecki, A. R., Brayer, G. D., Delbaere, L. T. J., & Bauer, C.-A. (1980) *J. Mol. Biol. 144*, 43-88.

Markley, J. L., & Ibanez, I. B. (1978) *Biochemistry 17*, 4627-4640.

Ringe, D., Petsko, G. A., Yamakura, F., Suzuki, K., & Ohmori, D. (1983) *Proc. Natl. Acad. Sci. U.S.A. 80*, 3879-3883.

Ringe, D., Seaton, B. A., Gelb, M. H., & Abeles, R. H. (1985) *Biochemistry 24*, 64-68.

Robertus, J. D., Alden, R. A., Birktoft, J. J., Kraut, J., Powers, J. C., & Wilcox, P. E. (1972) *Biochemistry 11*, 2439-2449.

Segal, D. M., Powers, J. C., Cohen, G. H., Davies, D. R., & Wilcox, P. E. (1971) *Biochemistry 10*, 3728-3738.

Sielecki, A. R., Hendrickson, W. A., Broughton, C. G., Delbaere, L. T. J., Brayer, G. D., & James, M. N. G. (1979) *J. Mol. Biol. 134*, 781-804.

Westkaemper, R. B., & Abeles, R. H. (1983) *Biochemistry 22*, 3256-3264.

NMR Study of the Molecular and Electronic Structure of the Heme Cavity of *Aplysia* Metmyoglobin. Resonance Assignments Based on Isotope Labeling and Proton Nuclear Overhauser Effect Measurements†

Usha Pande,‡ Gerd N. La Mar,*,‡ Juliette T. J. Lecomte,‡ Franca Ascoli,§ Maurizio Brunori,∥ Kevin M. Smith,‡ Ravindra K. Pandey,‡ Daniel W. Parish,‡ and V. Thanabal‡

Department of Chemistry, University of California, Davis, California 95616, Department of Experimental Medicine and Biochemical Sciences, University of Rome "Tor Vergata", 00173 Rome, Italy, and Department of Biochemical Sciences, CNR Center of Molecular Biology, University of Rome "La Sapienza", 00185 Rome, Italy

Received March 17, 1986; Revised Manuscript Received May 1, 1986

ABSTRACT: The ^{1}H NMR characteristics of the high-spin metmyoglobin from the mollusc *Aplysia limacina* have been investigated and compared with those of the myoglobin (Mb) from sperm whale. *Aplysia* metMb exhibits a normal acid ↔ alkaline transition with p$K \sim 7.8$. In the acidic form, the heme methyl and *meso* proton resonances have been assigned by ^{1}H NMR using samples reconstituted with selectively deuterated hemins and in the latter case by ^{2}H NMR as well. On the basis of the methyl peak intensities and shift pattern, heme rotational disorder could be established in *Aplysia* Mb; ~20% of the protein exhibits a reversed heme orientation compared to that found in single crystals. Three *meso* proton resonances have been detected in the upfield region between −16 and −35 ppm, showing that the chemical shift of such protons can serve as a diagnostic probe for a pentacoordinated active site in hemoproteins, as previously shown to be the case in model compounds. The temperature dependence of the chemical shift of the *meso* proton signals deviates strongly from the T^{-1} Curie behavior, reflecting the presence of a thermally accessible Kramers doublet with significant $S = {}^3/_2$ character. Nuclear Overhauser effect, NOE, measurements on *Aplysia* metMb have provided the assignment of individual heme α-propionate resonances and were used to infer spatial proximity among heme side chains. The hyperfine shift values for assigned resonances, the NOE connectivities, and the NOE magnitudes were combined to reach a qualitative picture of the rotational mobility and the orientation of the vinyl and propionate side chains of *Aplysia* metMb relative to sperm whale MbH_2O. Thus, it was found that the heme side chains are sterically less clamped in the former protein.

The myoglobin, Mb,[1] from the buccal muscle of the sea hare *Aplysia limacina* possesses several interesting properties that differentiate it from the more commonly studied mammalian Mbs. A number of structural and functional studies have

† This research was supported by Grants HL-16087 and HL-22252 from the National Institutes of Health and CU-84.01795.04 from the Consiglio Nazionale delle Ricerche.

‡ University of California.

§ University of Rome "Tor Vergata".

∥ University of Rome "La Sapienza".

[1] Abbreviations: Mb, myoglobin; metMb, metmyoglobin; Hb, hemoglobin; metHb, methemoglobin; NMR, nuclear magnetic resonance; NOE, nuclear Overhauser effect; Tris-HCl, tris(hydroxymethyl)aminomethane hydrochloride; Bis-Tris, 2-[bis(2-hydroxyethyl)amino]-2-(hydroxymethyl)-1,3-propanediol.

0006-2960/86/0425-5638$01.50/0

indicated that the most relevant substitution at the heme site responsible for the unique properties of this protein is the absence of a distal histidine (Tentori et al., 1971), which is substituted with a residue (probably a lysine) suggested to be partially turned out of the heme pocket toward the solvent (Bolognesi et al., 1985). Oxygen dissociation kinetics are about 7-fold more rapid (Wittenberg et al., 1965) than in horse heart Mb, in agreement with the structural findings. In addition, while the oxidized form of the protein appears to exhibit the usual alkaline–acid transition characteristic of other Mbs and Hbs, although at a slower rate (Giacometti et al., 1975), early optical studies (Rossi Fanelli & Antonini, 1957), azide binding kinetics (Giacometti et al., 1975), and ^{1}H NMR relaxation data (Giacometti et al., 1981) have all supported a five-coordinated ferric iron for the protein at acidic pH. Recent single-crystal X-ray data on *Aplysia* metMb confirms the absence of coordinated water (Bolognesi et al., 1985).

^{1}H nuclear magnetic resonance spectroscopy has been amply demonstrated to be one of the most powerful tools for elucidating functionally relevant structural properties of the heme cavity in hemoproteins, particularly in paramagnetic derivatives (La Mar, 1979; Satterlee, 1986). Structure-specific probes have been developed with model complexes that allow the unambiguous identification of several stereochemical and electronic properties of hemes in intact hemoproteins (La Mar & Walker-Jensen, 1978; La Mar, 1979). In each case, the structural probes have been found to be valid in proteins and have been used for informative comparisons among related proteins. The structural probe of interact here is that for differentiating between five-coordinated and six-coordinated high-spin ferric systems, for which model complexes display characteristically different hyperfine shift patterns for the *meso* protons. ^{1}H NMR data on model complexes (Budd et al., 1979) and sperm whale metaquoMb (La Mar et al., 1980a) have been shown to be consistent for the case of a six-coordinated iron(III). However, while the *meso*-H shifts have been used to infer five-coordination for modified sperm whale Mb (Morishima et al., 1985), there exists in the literature no example where the relevant NMR measurements have been carried out on a protein known to be five-coordinated on the basis of single-crystal X-ray data. Thus, *Aplysia* Mb (Bolognesi et al., 1985) serves as the ideal, and so far only, test case for the applicability of the structural probe in a myoglobin.

Other recently developed ^{1}H NMR structural probes allow for the detection of heme rotational disorder, where the heme occupies the two isomeric positions depicted in structures A and B of Figure 1; the two isomers differ by a 180° rotation about the α,γ-*meso* axis (La Mar et al., 1978, 1980b, 1983a,b). For mammalian Mbs, both isomers are populated at equilibrium (La Mar et al., 1983b), although the X-ray-defined orientation as in structure A in Figure 1 is strongly favored for native hemin (Takano, 1977). The influence of the distal histidine on this equilibrium is unknown, although the X-ray data on *Aplysia* Mb were found (Bolognesi et al., 1975) to be consistent with a single orientation (as in structure A of Figure 1). There are cases, however, where the two components are comparably populated in solution (La Mar et al., 1980b), even though only a single form is detected in the crystal (Steigemann & Weber, 1979). Lastly, very recent developments in the application of nuclear Overhauser effect (NOE) measurements (Noggle & Shirmer, 1971) in paramagnetic proteins have allowed the identification of signals from a heme side chain close to a heme methyl group (Unger et al., 1985). These assignments, in conjunction with the assignment of heme methyl peaks via isotope labeling, permit us to draw conclusions as to the relative orientations of propionate and vinyl side chains.

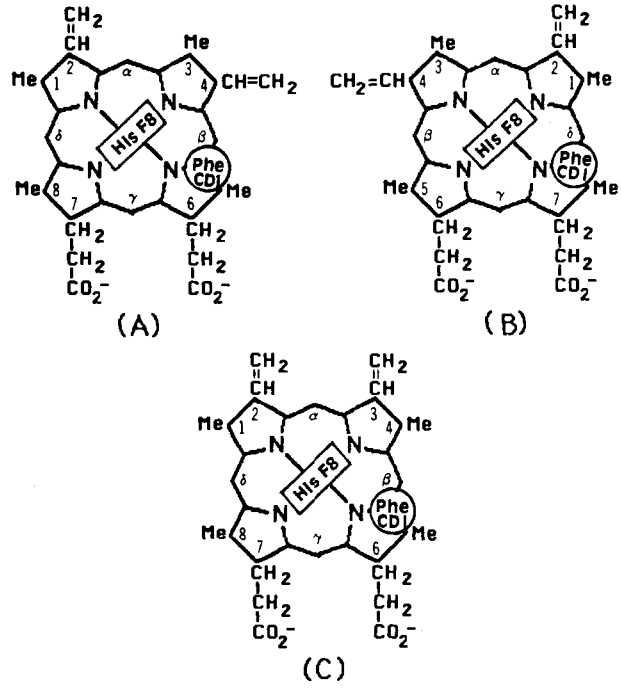

FIGURE 1: Heme orientation in *Aplysia* myoglobin viewed from the proximal side; (A) as found in the crystal structure (Bolognesi et al., 1985); (B) alternative orientation of the heme rotated 180° about the α,γ-*meso* axis; (C) protohemin III reconstituted into Mb; the positions of 3-CH_3 and 4-vinyl are interchanged in protohemin III, thereby making it symmetric about the α,γ-*meso* axis. The rectangle indicates the orientation of the imidazole π plane of proximal histidine F8 and the circle indicates the location of the ring of Phe-CD1.

We report herein on a high-field ^{1}H and ^{2}H NMR study of *Aplysia* metMb in the pH range 5.9–9.0 and draw parallels with sperm whale Mb well studied in our chosen pH range (Iizuka & Morishima, 1975; McGrath & La Mar, 1978; La Mar et al., 1980a). This study demonstrates the validity of the nature of the *meso*-H hyperfine shift as an indicator of the presence or absence of water at the sixth position of a ferric hemoprotein, establishes the presence of appreciable heme rotational disorder, supports a significant contribution of intermediate-spin character to thermally accessible states, and provides qualitative comparisons on the orientations and internal mobilities of side chains relative to those in sperm whale Mb.

Experimental Procedures

Aplysia Mb was prepared from the buccal muscle of the mollusc *Aplysia limacina* (collected in the Mediterranean sea near Naples) as described by Rossi Fanelli and Antonini (1957). After the last precipitation in 98% saturated ammonium sulfate, the red precipitate was dissolved in water and centrifuged to remove some undissolved material, and the solution was freed from ammonium sulfate either by extensive dialysis or by passage through a Sephadex G-25 column equilibrated with the desired buffer. The protein so obtained contains less than 5% of a minor component, as revealed by analytical electrofocusing. The ferric protein was prepared by addition of a 2-fold excess of potassium ferricyanide in 0.1 M Tris-HCl buffer, pH 8.0, followed by dialysis to remove the excess oxidant and the product ferrocyanide. Concentration of the ferric protein was determined spectrophotometrically at 505 nm (ϵ = 13 100 M^{-1} cm^{-1} at pH 6.0) (Rossi Fanelli & Antonini, 1957). Native Mb was finally stored in 98% saturated ammonium sulfate solution. A fraction of this

Mb was further purified by preparative electrofocusing (pH range 3.5–5.2), followed by extraction of the main red band with buffer and centrifugation. Ammonium sulfate was added to the supernatant up to 95%, and the precipitate was dissolved in 2 mM Bis-Tris buffer, pH 7.0, and dialyzed against the same buffer.

Aplysia apomyoglobin was obtained from the native protein (yield about 70%) by using the modified acid–acetone method described elsewhere (Rossi Fanelli & Antonini, 1957). Protein concentration was determined spectrophotometrically [ϵ_{280} = 13 000 M^{-1} cm^{-1} (Rossi Fanelli & Antonini, 1957)]. Protohemin III and protohemins IX deuterated specifically at the *meso*-$^2H_4$, 1,3-$(C^2H_3)_2$, 1,5-$(C^2H_3)_2$, and 8-C^2H_3 positions were employed for the reconstitution of the holoprotein. These hemins are the same as those reported previously (Smith et al., 1979, 1983, 1986; Parish, 1984). Apomyoglobin was reconstituted with protohemin III and specifically deuterated protohemins IX according to the reported procedure (Ascoli et al., 1981); 0.5 mg of each hemin was dissolved in a minimum volume of 0.01 M NaOH in H_2O and added to 14 mg of globin in 2 mM Bis-Tris-HCl buffer in H_2O (pH 6.7). The sample was kept at 10 °C for several hours to equilibrate and centrifuged to remove any precipitate.

An aliquot of ferric *Aplysia limacina* Mb [suspension in 98% $(NH_4)_2SO_4$ solution] was centrifuged and the supernatant discarded. The pellet was dissolved in 2 mM Bis-Tris-HCl buffer (pH 7.0). This *Aplysia* Mb solution was then passed through a Sephadex G-25 column preequilibrated with Bis-Tris-HCl buffer (2 mM, pH 7). The resulting eluate was concentrated to a minimum of 2 mM protein in an Amicon ultrafiltration cell with a YM5 membrane. All samples were exchanged with several volumes of Bis-Tris-HCl buffer (2 mM) in ^2H_2O (for ^1H NMR measurements) or in deuterium-depleted water (for ^2H NMR measurements). The sample pH was adjusted with 0.2 M NaO^2H (NaOH) or ^2HCl (HCl). The pH was measured with a Beckman 3550 pH meter equipped with an Ingold 620 microcombination electrode; pH values were uncorrected for the isotope effect and therefore will hereafter be denoted as pH* in the case of ^2H_2O samples.

^1H NMR spectra were recorded on a Nicolet NT-360 FT NMR spectrometer operating at 360 MHz in the quadrature mode. Data were collected by using double precision on 16 384 data points over an 80-kHz bandwidth. The 90° pulse was 7 μs. Typical spectra consisted of 2000–10 000 transients except for NOE measurements. The nuclear Overhauser spectra were recorded by applying a decoupler presaturation pulse of 30 ms to the desired resonance. Corresponding reference spectra were collected under identical conditions but with the decoupler pulse off-resonance. On- and off-resonance frequencies were alternated every 512 scans (Unger et al., 1985). The NOE spectra consisted of 30 000 transients with a repetition rate of 11.8 s^{-1}. The signal-to-noise ratio was improved by apodizing the free induction decays; this data treatment introduced 30-Hz line broadening. Account was taken of the artificial line broadening in all calculations.

A ^2H NMR spectrum of a 1 mM solution of [α,β,γ,δ-*meso*-$^2H_4$]hemin reconstituted *Aplysia* metMb was recorded on a Nicolet NT-500 FT NMR spectrometer with a deuterium probe operating at a frequency of 76.76 MHz. The spectrum was collected by using double precision on 8192 data points over a 34-kHz bandwidth; the 90° pulse was 27 μs. The spectrum consisted of 5 × 10^5 transients collected at a repetition rate of 16.7 s^{-1}. The FID was apodized at 100 Hz.

Chemical shifts for all spectra are referenced to DSS (2,2-dimethyl-2-silapentane-5-sulfonate) through the residual water signal. The line widths and areas of peaks were measured by using the NMCCAP curve-fitting program available on the Nicolet 1280 data system.

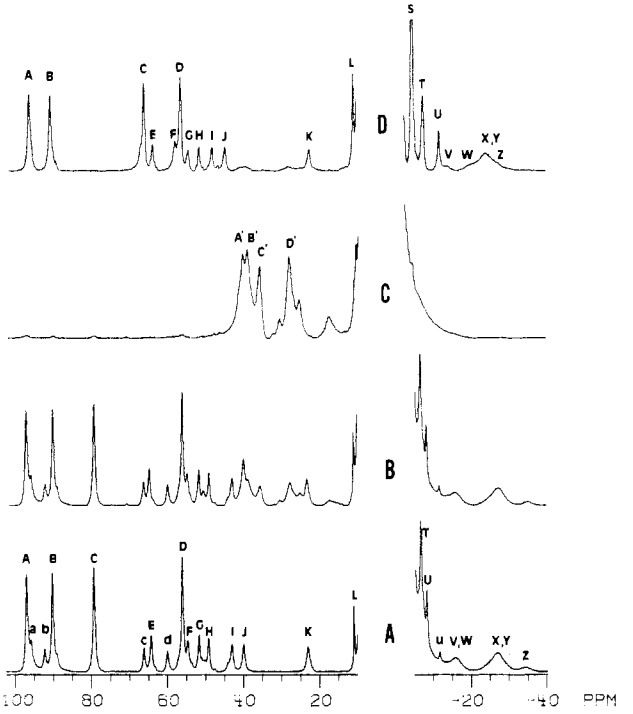

FIGURE 2: Hyperfine-shifted portions of the 360-MHz ^1H NMR spectra of *Aplysia* metMb in ^2H_2O and 2 mM Bis-Tris-HCl buffer at 25 °C for native protein at pH* 5.9 (A), 7.4 (B), and 9.0 (C). The spectrum of the protein reconstituted with protohemin III at pH* 6.6 and 25 °C is illustrated in (D).

RESULTS

Comparison with Sperm Whale Mb. The resolved portions of the hyperfine shifted regions of the 360-MHz ^1H NMR spectra of *Aplysia* metMb at pH 5.9, 7.4, and 9.0 are illustrated in traces A–C of Figure 2, respectively. The spectra at low pH resemble those of sperm whale metMbH_2O (Iizuka & Morishima, 1975; McGrath & La Mar, 1978; La Mar et al., 1980a). Particularly prominent are four apparent methyl peaks in the region 50–100 ppm, with line widths of ~200 Hz at 25 °C, some 30% lower than in sperm whale Mb. As the pH is raised, the peaks lose intensity at the expense of a new spectrum which emerges in the region 40–10 ppm. The spectrum at high pH is remarkably similar to that of sperm whale (McGrath & La Mar, 1978) or horse (Iizuka & Morishima, 1975) metMbOH. Integration of the areas of methyl peaks for the two forms yields a pK ~7.8, close to the value determined optically for the acid ↔ alkaline transition (Giacometti et al., 1975). It may be noted that *Aplysia* metMb exhibits well-resolved and separate signals for the acidic and alkaline forms, with no detectable line broadening at the pK for either species. This is in sharp contrast to sperm whale metMbH_2O, where intermediate exchange conditions prevailed (McGrath & La Mar, 1978), and dictates (Carrington & McLachlan, 1967) that the rate of the acid–alkaline transition in *Aplysia* metMb is $\ll 1.5 \times 10^2$ s^{-1}, at least 3 orders of magnitude slower than for sperm whale metMb (Ilgenfritz & Schuster, 1971; McGrath & La Mar, 1978). These results are in agreement with previous findings on the relaxation time of the acid–alkaline transition of *Aplysia* metMb (Giacometti et al., 1975).

Analysis of the *Aplysia* metMb spectrum at pH* 5.9 (Figure 2, trace A) reveals a set of 11 resolved low-field

Table I: ^{1}H NMR Parameters for Resolved Resonances in *Aplysia* Metmyoglobin and Metmyoglobin Hydroxide[a]

peak	assignment[d]	*Aplysia* metMb[b] chemical shift (ppm)	line width (Hz)	no. of protons[e]	intercept[f] (ppm)	sperm whale metMbH$_2$O[c] chemical shift (ppm)
A	8-CH_3	96.8	200 ± 20	3	5.3	91.7
B	5-CH_3	90.0	200 ± 20	3	6.5	84.9
C	3-CH_3	79.0	200 ± 20	3	−4.2	73.2
D	1-CH_3	55.8	200 ± 20	3	7.4	53.2
E	7-α-CH	64.0	210 ± 10	1	10.9	75.5
F	6-α-CH	54.4	220 ± 40	1	6.1	59.2
G	4-α-CH[g]	51.5	200 ± 30	1	9.4	46.4
H	6-a-CH	48.9	200 ± 20	1	15.9	44.9
I	7-α-CH	42.8	220 ± 60	1	3.5	30.9
J	2-α-CH[g]	39.7	230 ± 60	1	13.2	31.4
K		22.8	250 ± 50	1	19.0	
L		10.7	80 ± 20	1	10.7	
T		−7.1	350 ± 40	8–9	11.5	
U	4-β-CH[g]	−8.6	150 ± 50	1	5.4	
V		−16.1	1000 ± 200	~1	20.0	
W	*meso*-H	−16.6	900 ± 200	~1	−18.4	
X	Val-E11 γ-CH_3	−27.2	1000 ± 300	~3	21.2	
Y	*meso*-H	−29.4	850 ± 200	~1	−28.4	
Z	*meso*-H	−34.4	990 ± 200	~1	−20.8	
a	5-CH_3[h]	95.6	200 ± 30	0.65	5.2	89.1[h]
b	8-CH_3[h]	92.1	200 ± 30	0.65	2.1	86.1[h]
c	1-CH_3[h]	65.9	200 ± 30	0.65	3.4	54.3[h]
d	3-CH_3[h]	59.7	200 ± 30	0.65	2.8	65.6[h]
u		−12.0	200 ± 40	~0.20	15.0	

peak	assignment[d]	*Aplysia* metMbOH[i] chemical shift (ppm)	line width (Hz)	no. of protons	intercept (ppm)	sperm whale metMbOH[j] chemical shift (ppm)
A′	heme methyl	39.6	430 ± 50	~3	14.1	35.2
B′		38.5	450 ± 50	~3	21.6	35.2
C′		35.2	450 ± 50	~3	20.2	31.7
D′		27.4	450 ± 50	~3	13.3	25.0

[a] In ^2H_2O and 2 mM Bis-Tris-HCl at 25 °C, the chemical shifts are referenced to DSS through the residual water signal. [b] *Aplysia* metMb data reported at pH* 5.9. [c] Sperm whale metMbH$_2$O data at pH* 6.2, taken from La Mar et al. (1980a) and Unger et al. (1985). [d] Assignments for heme protons based on isotope labeling and NOEs. [e] Peak area normalized to A (8-CH_3) as three protons. [f] Intercept at $T^{-1} = 0$, in ppm from DSS, obtained from Figure 3. [g] Assigned by analogy to sperm whale metMbH$_2$O (see text). [h] Methyl peak corresponding to reversed heme orientation as in structure B of Figure 1; data for sperm whale metMbH$_2$O taken from Davis (1982). [i] *Aplysia* metMbOH data obtained at pH* 9.0. [j] Sperm whale metMbOH data taken from McGrath and La Mar (1978).

resonances which have relative intensities 1 or 3, just as found for sperm whale metMbH$_2$O (La Mar et al., 1980a); these peaks are labeled A–K. Other peaks that can be associated with the same protein complex are single proton peaks L and U–Z, methyl peak X, and peak S which must contain several methyl groups. The chemical shifts, line widths, and areas in terms of number of protons are listed in Table I for all resolved resonances. Closer inspection of trace A in Figure 2 reveals, however, additional peaks with less than unit proton intensity. Several of these peaks must arise from another isozyme or an impurity (shoulders at 88.5, 63.0, 50.5, and 48.0 ppm), since these intensities are significantly reduced in the exhaustively purified sample (compare trace A of Figure 2 with that of Figure 4). Note, however, that several low-intensity peaks remain unaltered in Figure 4A, indicating that a conformational heterogeneity for a single polypeptide chain may be present. Of these, four equally intense peaks are labeled a–d, each of which comprises 0.65 proton when scaled to peaks A–D as methyls or E–K as single protons. There is evidence of additional peaks of ~0.2 proton intensity near 53.3, 50.0, and 43.8 ppm (not labeled). In the upfield region, only one peak is identified with ~0.2 proton intensity, peak u.

The trace of *Aplysia* metMb reconstituted with the symmetric hemin III (part C in Figure 1), illustrated in trace D of Figure 2, exhibits essentially one set of peaks with all peak areas either one (E–K) or three protons (A–D) in the low-field region. Some evidence of heterogeneity is due to impurities in the apoprotein preparation (see shoulders to peaks B and C). Similar peaks were detected in native preparations but could be suppressed by exhaustive purification. The upfield region shows the same peaks as in native protein, except that peak u is missing. The most striking differences between native and hemin III–metMb are the large changes in the shift of a single methyl (peak C shifts from 79 to 66 ppm) and a narrow single proton peak U (which shifts from −8.6 to −12.0 ppm). Since the two hemins differ solely in the interchange of the 3-CH_3 and 4-vinyl, the shift changes argue strongly for peak C arising from the 3-CH_3 in the native and the 4-CH_3 in the hemin III–metMb, while peak U must originate from the 4-vinyl and the 3-vinyl H_βs, respectively. The H_β(trans) of heme vinyls are known to resonate upfield of DSS in both model compounds (Budd et al., 1979) and sperm whale metMbH$_2$O (La Mar et al., 1980a).

The influence of temperature on the hyperfine shifts of resolved resonances in acidic *Aplysia* metMb as well as metMbOH is illustrated in Figure 3 in a plot of observed shift vs. reciprocal temperature [Curie plot (Jesson, 1973)]. All data points yield straight lines, and the intercepts at $T^{-1} = 0$ are listed in Table I. In contrast to sperm whale metMbH$_2$O, for which all heme peaks yielded intercepts close to their diamagnetic positions (La Mar et al., 1980a), *Aplysia* metMb has several peaks in the upfield region which exhibit gross deviations from Curie behavior. The prominent peaks for *Aplysia* metMbOH, which must arise from heme methyls

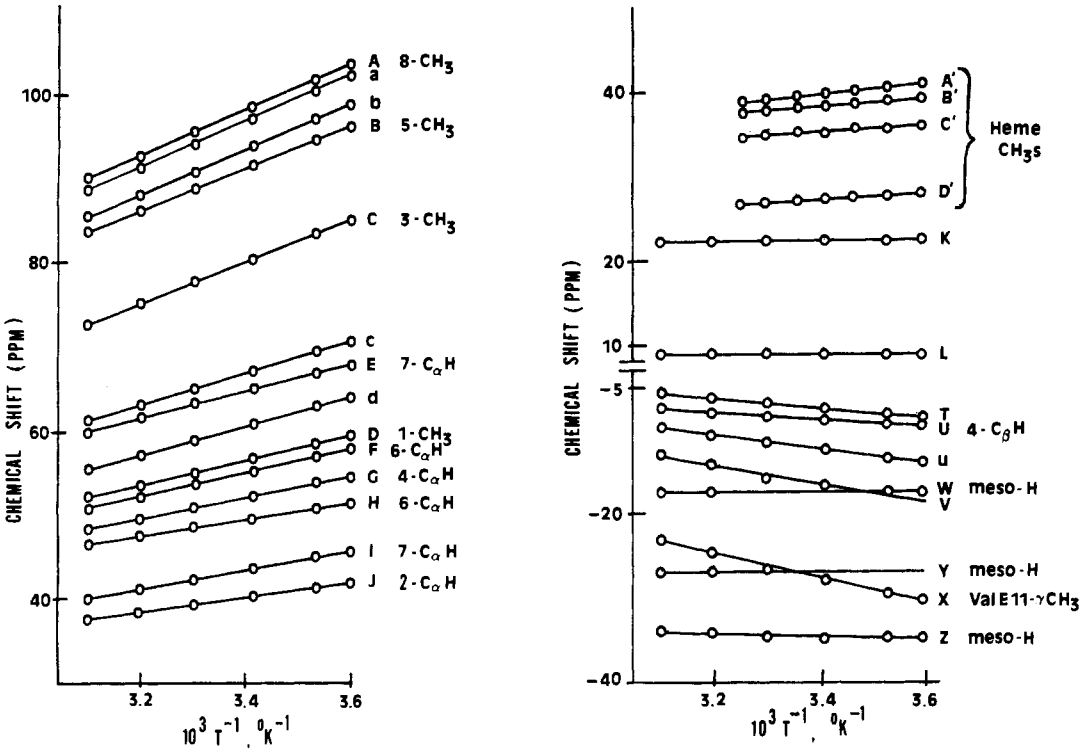

FIGURE 3: Plot of chemical shift vs. reciprocal temperature (Curie plot) for all resolved resonances A–L, T–Z, a–d, and u in *Aplysia* metMb at pH* 5.9 and for heme methyls A′–D′ in metMbOH at pH* 9.0. The intercept at $T^{-1} = 0$ for each line is given in Table I.

(McGrath & La Mar, 1978), exhibit deviations from Curie behavior very similar to those observed for the heme methyls of the analogous sperm whale derivative (Iizuka & Morishima, 1975). These deviations reflect the known high-spin/low-spin equilibrium characteristic of all met–hydroxy complexes of Mb and Hb (Antonini & Brunori, 1971).

Peak Assignments via Isotope Labeling. The assignment of individual methyl groups in acidic metMb is illustrated in Figure 4, where we compare the downfield traces of the native protein (trace A) with that of the proteins reconstituted with hemins possessing deuterated methyls at positions 1 and 3 (trace B), positions 1 and 5 (trace C), and position 8 (trace D). The presence of two species is clearly confirmed in each trace by the reduced intensities of two peaks per deuterated methyl group, one from the set A–D and the other from the set a–d. The resulting assignments are given for each peak in Table I. This definitively establishes the presence of molecular heterogeneity, with the relative areas of methyls A–D to methyl a–d giving a ratio of components as 4.5:1.

The location and identification of the *meso*-H resonances are presented in Figure 5. Inspection of trace A for the native protein at 50 °C (which considerably improves resolution over 25 °C without denaturation of the protein) (Brunori et al., 1968) reveals more clearly several broad single proton peaks, V, W, Y, and Z, of which at least W, Y, and Z exhibit substantially reduced intensities in the protein reconstituted with [$\alpha,\beta,\gamma,\delta$-*meso*-$^2H_4$]hemin (trace B). Thus, peaks W, Y, and Z must arise from three of the four *meso* protons in the major component; the fourth signal is probably under the severe shoulder from the diamagnetic envelope. The location of *meso*-H signals in the upfield region is confirmed by direct detection of the labels by ^2H NMR, at 25 °C as shown in trace C of Figure 5. In spite of the broad diamagnetic envelope, two of the *meso*-^2H peaks are clearly resolved at −29 and −34 ppm (note in Figure 3 that the *meso*-H hyperfine shifts are essentially temperature independent). Significance is attributed not only to the ^2H NMR detection of *meso* proton resonances upfield but also to the complete absence of such peaks in the downfield region where these peaks resonate in six-coordinate metMbH_2O (La Mar et al., 1980a).

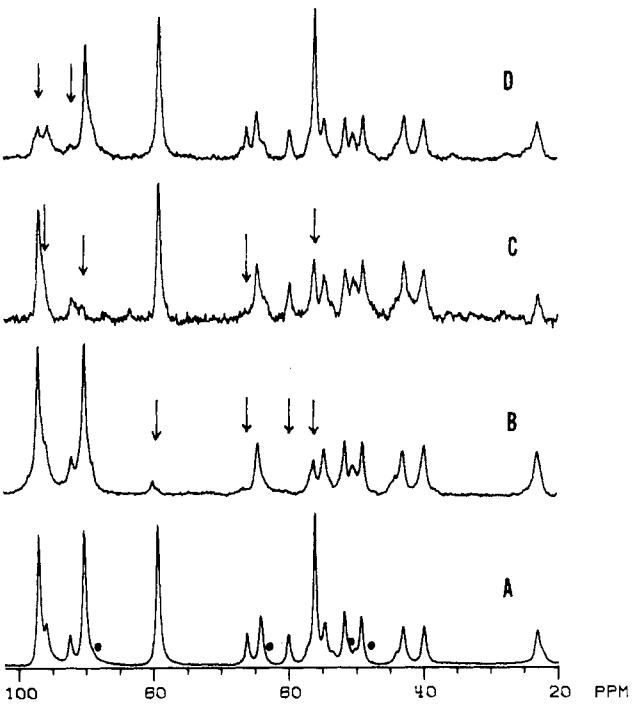

FIGURE 4: Assignment of downfield-shifted heme methyl resonances in *Aplysia* metMb in ^2H_2O and 2 mM Bis-Tris-HCl and 25 °C. (A) Native exhaustively purified metMb, pH* 6.0; (B) reconstituted metMb using 1,3-$(C^2H_3)_2$-hemin, pH* 6.6; (C) reconstituted metMb using 1,5-$(C^2H_3)_2$-hemin, pH* 6.6; (D) reconstituted metMb using 8-(C^2H_3)-hemin, pH* 6.6. The vertical arrows in each trace indicate the heme methyl resonances with reduced intensities because of selective deuteration. The filled circles in (A) indicate the positions where small peaks attributable to heterogeneity disappeared after extensive purification of the native protein by preparative electrofocusing and exhaustive dialysis.

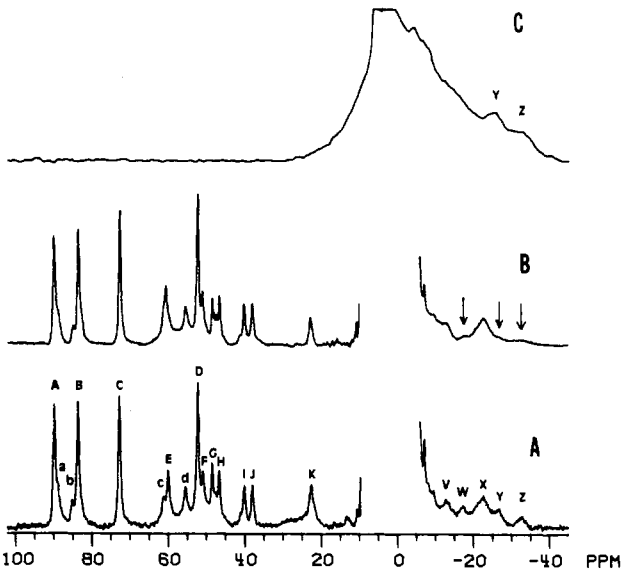

FIGURE 5: Assignment of resolved *meso*-H resonances in reconstituted *Aplysia* metMb by ^1H and ^2H NMR. (A) ^1H NMR spectrum of native metMb at pH* 6 in ^2H_2O and 2 mM Bis-Tris-HCl at 50 °C; (B) ^1H NMR spectrum of metMb reconstituted with [*meso*-$^2H_4$]-hemin, at pH* 6 in ^2H_2O and 2 mM Bis-Tris-HCl at 50 °C; (C) ^2H NMR spectrum of metMb reconstituted with [*meso*-$^2H_4$]hemin at pH* 7 and 25 °C in H_2O. The vertical arrows in (B) show the positions where resonance intensities decreased owing to deuteration.

Peak Assignments via Nuclear Overhauser Effect Measurements. The spectral data in Figure 6 represent the reference spectrum for native *Aplysia* metMb (trace A) and the difference spectra obtained upon saturating a series of individual peaks (traces B–F). Thus, irradiation of peak A (8-CH_3) yields a −0.5% NOE solely to peak E (trace B). Conversely, saturation of peak E leads to the expected reciprocal NOE to peak A as well as a −4.4% NOE to peak I (trace C); saturating peak I yields a −10% NOE to peak E (trace D). This same pattern of NOEs has been observed in sperm whale metMbH_2O (Unger et al., 1985) and was shown to be consistent with expectations on the basis of relative distances and spin–lattice relaxation times. Thus, the NOE connectivities between peaks A, E, and I point directly toward peaks E and I originating from the 7-α-methylene protons, with peak E closer to the 8-CH_3 than peak I. Similarly, saturation of peak B (5-CH_3) yields a −0.5% NOE solely to peak H (trace E). When peak H is saturated, it yields a small NOE to peak F as well as the reciprocal NOE to peak B (trace F). Mapping the off-resonance effects as a functional of decoupler offset demonstrates that the intensity of peak F in the difference spectrum (Figure 6F) is mainly due to NOE from peak H, whereas that of peak D can be accounted for entirely by off-resonance saturation. Thus, peaks H and F arise from the 6-α-methylene protons, with peak H closer to 5-CH_3. The saturation of methyl peaks 1 and 3 (peaks C and D) failed to yield detectable NOEs to any resolved peaks; in particular, no NOE was observed to the 4-vinyl H_β (peak U). Such NOEs showing the proximity of 3-CH_3 and 4-H_β as well as 1-CH_3 and 2-H_β were clearly observed in metMbH_2O (Unger et al., 1985).

Saturating the remaining three low-field peaks, G, J, and K, failed to yield any detectable NOE (<−0.2%) to any other resolved peak. Of these three peaks, two must originate from the two vinyl H_αs and the third presumably from the β-methylene group of the proximal histidine. On the basis of strong similarities of methyl and methylene hyperfine shifts in *Aplysia* metMb and sperm whale metMbH_2O (La Mar et al., 1980a) (compare data in Table I), we tentatively assign

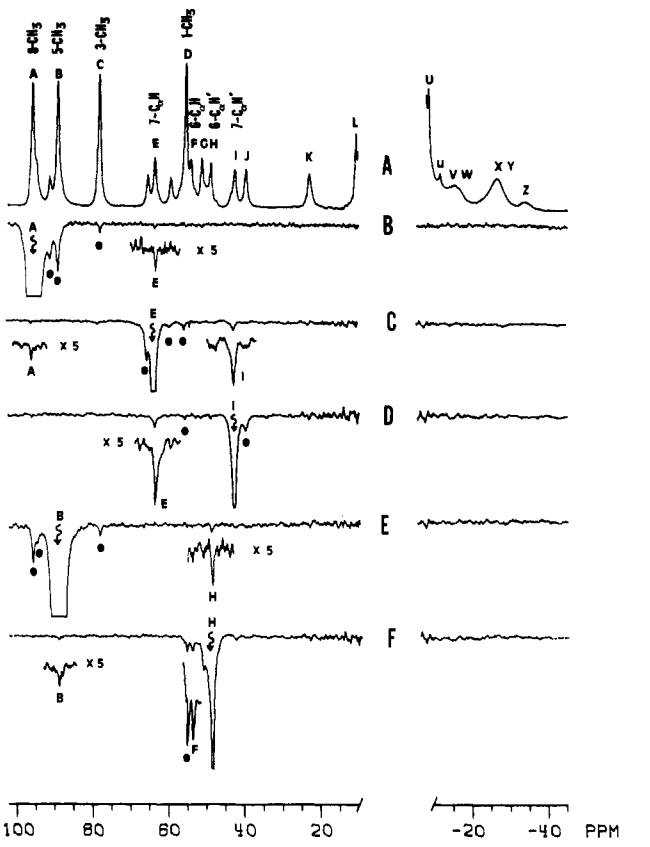

FIGURE 6: Resolved portions of the 360-MHz ^1H NMR spectra of *Aplysia* metMb in ^2H_2O and 2 mM Bis-Tris-HCl at 30 °C and pH* 5.9. (A) Reference spectrum; (B–F) are the NOE difference spectra resulting from saturation of desired resonance by a 30-ms, 50-mW decoupler pulse; spectra intensity 5× that of (A). For a given difference spectrum, two spectra were obtained in an interleaved fashion: the first spectrum with saturation pulse on the peak of interest and the second under identical experimental conditions but with the saturation pulse set off-resonance to provide the reference spectrum (Unger et al., 1985). (B) Saturation of peak A (8-CH_3) showing an NOE to peak E (7-α-CH); (C) saturation of peak E (7-α-CH) showing NOE to peaks A (8-CH_3) and I (7-α'-CH); (D) saturation of peak I (7-α'-CH) showing NOE to peak E (7-α-CH); (E) saturation of peak B (5-CH_3) showing NOE to peak H (6-α'-CH); (F) saturation of peak H (6-α'-CH) showing NOE to peaks B (5-CH_3) and F (6-α-CH). In each of the difference spectra B–F, an arrow (⟿) indicates the peak being saturated, and filled circle (●) denotes the peak whose intensity can be accounted for in full by off-resonance saturation due to power spillage.

peak G to the 4-H_α and peak J to the 2-H_α. These signals could be assigned on the basis of isotope labeling in the latter protein and resonate with chemical shifts very close to peaks G and J. Although *meso*-H's are very close to the adjacent pyrrole methyls, the very short relaxation times for *meso*-H's due to their proximity to the iron (La Mar & Walker-Jensen, 1978) preclude the detection of NOEs for these peaks.

Discussion

Molecular Heterogeneity and Heme Rotational Disorder. The ^1H NMR traces for highly purified native *Aplysia* metMb (trace A in Figure 4) are indicative of molecular heterogeneity. The major component (~82%) gives rise to the set of signals A–Z and the minor component the methyl signals a–d. The difference between the two components lies in the environments of individual pyrrole rings and is reflected by the appended methyl hyperfine shift interchanged as 1-CH_3 ↔ 3-CH_3 and 5-CH_3 ↔ 8-CH_3. This is the same interchange of environments as was observed in sperm whale metMb (Jue et al., 1983; Davis, 1982; La Mar et al., 1983b), and for which the

origin of the two sets of signals could be unambiguously attributed (Lecomte et al., 1985) to the two heme rotational isomers depicted in structure A and B of Figure 1. The methyl hyperfine shift pattern for the major component of *Aplysia* and sperm whale metMb are the same, in that the 8-CH_3 is at lower field than the 5-CH_3 (see Table I). The minor components for these two proteins have these two methyl positions reversed. Thus, the heme orientation in the major components is the same in *Aplysia* and sperm whale Mbs (structure A in Figure 1). While this conclusion has already been deduced from the preliminary X-ray structure (Bolognesi et al., 1985), only a single form could be detected in the solid state.

Thus, the heme orientational disorder is more extensive in *Aplysia* than in the characterized mammalian Mbs, as the equilibrium proportion of the minor isomer with the heme orientation as in structure B of Figure 1 is approximately twice as abundant in the *Aplysia* protein.

Structural Probe for Ligated Water. In spite of remarkable similarities in the downfield portions of the ^1H NMR traces of *Aplysia* and sperm whale metMb involving the pyrrole substituents, the overall hyperfine shift patterns differ dramatically for the *meso*-H shifts. The exact electronic origin of the difference in *meso*-H shifts is not yet clear, but there are no exceptions to the correlation among the characterized models and proteins. Thus, while pyrrole substituents show very similar hyperfine shifts for five- and six-coordinated high-spin ferric complexes (Budd et al., 1979; La Mar & Walker-Jensen, 1978), the *meso*-H shifts are characteristically downfield (~40 ppm) for the six-coordinate systems and upfield (−20 to −50 ppm) for the five-coordinate systems. Both the ^1H NMR and ^2H NMR spectra for *Aplysia* metMb, as demonstrated in Figure 5, clearly show the absence of downfield *meso*-H signals and locate three of the four *meso*-H peaks in the region −16 to −35 ppm. This highly satisfactory correlation between ferric ion coordination number in both models and proteins establishes this as a useful diagnostic probe for ligated water in Mbs and Hbs and potentially as a general probe for high-spin ferric ligation state in hemoproteins not necessarily possessing an axial histidine.

Electronic Structure of the Heme Iron. While the low-field heme methyl (50–90 ppm) and upfield *meso*-H (−16 to −35 ppm) shifts are clearly indicative of a basically five-coordinate, high-spin ferric state, the shifts alone do not determine the purity of the ground spin state. Ferric hemes in purely high-spin five- or six-coordinate forms exhibit essentially Curie behavior (Jesson, 1973; La Mar & Walker-Jensen, 1978) for all heme resonances arising from substituents which themselves are not undergoing temperature-dependent changes in orientations. This dictates that the intercepts of Curie plots occur very close to the diamagnetic position for the orientationally fixed functional groups. Such behavior has been found in most model compounds (Budd et al., 1979; La Mar & Walker-Jensen, 1978) and in sperm whale metMbH_2O (La Mar et al., 1980a). Thus, deviations from Curie behavior in the present system must have their origin either in an equilibrium between different spin states (heme methyls and *meso*-H are the ideal probes) or, if detected only for selected pyrrole substituents, in the internal mobility for the side chain (propionate and/or vinyl groups).

For the high pH form of *Aplysia* metMbOH (as also found for mammalian metMbH_2O) (Iizuka & Morishima, 1975), the dominant methyl (peaks A′, B′, C′ and D′) shifts exhibit clear deviations from T^{-1} behavior in the direction of shifts increasing more slowly than T^{-1} as the temperature is lowered. This is readily attributed to the increased population of the $S = {}^1/_2$ ground state, which exhibits much smaller shifts than the excited $S = {}^5/_2$ state (La Mar & Walker-Jensen, 1978). Thus, the magnetic properties of the alkaline form of *Aplysia* metMb are completely consistent with hydroxy ligation (Antonini & Brunori, 1971).

The pH* 5.9 form of *Aplysia* metMb exhibits much more complicated temperature dependencies for its various resonances. As illustrated in the Curie plot in Figure 3, while all peaks yield straight lines, the degree of adherence to the Curie law (i.e., proximity of intercepts at $T^{-1} = 0$ near the diamagnetic position) varies dramaticaly with the considered resonance. For the known heme signals, the downfield signals generally adhere much more closely to the Curie law than the upfield *meso*-H resonances. The *meso*-H deviations are dramatic and must reflect the contributions from states other than a pure $S = {}^5/_2$ state at ambient temperatures. That the ground-state Kramers doublet is essentially pure ${}^5/_2$ has been established by the normal $g = 6$, 2 values in the low-temperature electron spin resonance spectrum (Rotilio et al., 1971). Similar systematic deviations from Curie law for particularly the *meso*-H resonances have been found (Goff & Shimomura, 1980) for a five-coordinate model complex for which a strong spin-quartet admixture to excited Kramers doublets was proposed. In this case the importance of the spin-quartet contribution to the ambient temperature properties could be demonstrated through a reduced magnetic moment relative to that of a pure high-spin complex (Reed et al., 1979). The reason that the deviations from the Curie law are more readily seen for the *meso*-H shifts than for any pyrrole substituent shift is because the latter hyperfine shifts are less sensitive to the spin state than the *meso*-H shifts. Thus, we conclude that *Aplysia* metMb possesses a thermally accessible Kramers doublet with significant $S = {}^3/_2$ character. It is noteworthy that horseradish peroxidase (Leigh et al., 1975) as well as ferricytochrome *c*′ (Maltempo et al., 1974; La Mar et al., 1981), both of which are five-coordinate with an axial histidine, have been proposed to possess important spin-quartet contributions to their electronic structures.

Although the four methyls exhibit essentially Curie behavior, several of the single proton resonances appear to present some selective deviations which might reflect temperature-dependent rotational changes. Thus, two of the four propionate α-CH's (peaks E and H), have rather large downfield intercepts. It has been noted that the structurally stabilizing salt bridges involving the propionate carboxylates are missing in *Aplysia* when compared with sperm whale Mb, and possible rotational disorder for propionates has been suggested (Bolognesi et al., 1985). Both of the signals tentatively assigned to the two vinyl H_αs (peaks G and J) also show rather low-field intercepts and thus also suggest sterically less clamped vinyls in *Aplysia* than in sperm whale metMb. These structural findings are fully consistent with a lower heme–apoprotein affinity in *Aplysia* myoglobin, compared to mammalian myoglobins, as suggested by experiments of heme transfer described by Rossi Fanelli and Antonini (1960).

Several of the hyperfine-shifted peaks necessarily of protein origin also exhibit intercepts outside their likely diamagnetic positions, although few assignments are firm here. This, however, is expected, inasmuch as the hyperfine shift for noncoordinated side chains originate solely from the small dipolar contribution to the shift with its necessarily T^{-2} dependence (Jesson, 1973; La Mar & Walker-Jensen, 1978). For the heme (and proximal histidine) resonances, the strong dominance of the contact shift with its T^{-1} dependence is

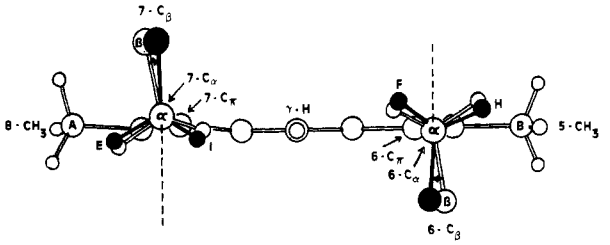

FIGURE 7: Projection of the heme propionate groups relative to the heme plane for sperm whale metMbH_2O as determined from available X-ray coordinates (open circles) (Takano, 1977). The view shown is looking directly at the heme edge along the α,γ-*meso* axis. The combination of NOE assignments and relative magnitudes of α-CH contact shifts determine qualitatively the direction in which the propionates are rotated in *Aplysia* metMb (dark circles) relative to those in sperm whale metMbH_2O. The magnitude of the rotations depicted are not significant. C_π designates the pyrrole aromatic carbons, C_6 and C_7. The carboxyl group and β-protons of each propionate are omitted for clarity. The letters indicate the protons as identified by their label in trace A of Figure 2.

expected for a single state. The very large line width of the upfield three-proton signal, X, suggests that it arises from a γ-CH_3 of Val-E11, which the X-ray structure places only 4 Å from the iron (Bolognesi et al., 1985). A similarly broad upfield peak has also been assigned to the same residue in sperm whale metMbH_2O (La Mar et al., 1980a). The upfield bias is attributed to dipolar shifts connected to the large zero-field splitting in high-spin ferric hemes (La Mar & Walker-Jensen, 1978).

Orientation of Heme Side Chains. The preliminary X-ray data indicate that the two propionates are oriented qualitatively similarly in *Aplysia* and sperm whale Mb, in that the carboxylates appear to point to the distal and proximal sides of the heme pocket for the 6- and 7-propionate groups, respectively (M. Bolognesi, private communication). Quantitative conclusions as to the propionate orientations in the single crystal of *Aplysia* metMb, however, are not yet possible owing to, in part, the presence of heme disorder and to some inconsistencies with published sequence data (Tentori et al., 1971).

The predominantly contact origin or the heme substituent hyperfine shifts in the present sytem allows some qualitative interpretations of the propionate α-methylene shifts in terms of the orientation of the C_π–C_α bonds in *Aplysia* relative to those in sperm whale metMb (Figure 7). The magnitude of the contact shift for an α-CH attached to a π system is given by the relation (La Mar, 1973):

$$(\Delta H/H)_{con} = A \cos^2 \phi$$

where A is a constant and ϕ is the dihedral angle between the C_π–C_α–H plane and the $C_\pi p_z$ axis. Thus, similar contact shifts for a pair of methylene protons indicate a symmetric disposition of the two protons with respect to the normal to the heme plane (i.e., the C_α–C_β bond projection in Figure 7 would be perpendicular to the heme plane). For 7-α-CH_2 in *Aplysia* MetMb, peaks E and I exhibit quite dissimilar contact shifts, with E (the proton closer to 8-CH_3) possessing the larger shift. Thus, the C_α–C_β bond projection must tilt toward the 8-CH_3, as illustrated in Figure 7. Moreover, since the difference in the two 7-α-CH contact shifts is smaller in *Aplysia* than sperm whale metMb (with the same mean shift), we can conclude that this C_α–C_β bond projection is rotated slightly clockwise in *Aplysia* as compared to sperm whale metMb, as depicted in Figure 7. For the 6-α-methylene group, as in sperm whale metMbH_2O, the two α-CH contact shifts are very similar, indicating a much more symmetric orientation. However, while the sperm whale metMbH_2O the proton nearest the 5-CH_3 shows the larger contact shift (Unger et al., 1985), the proton with the smaller contact shift is closer to the 5-CH_3 in *Aplysia* metMb. This suggests that the C_α–C_β bond projection for 6-propionate tilts slightly in the clockwise direction from the normal (Figure 7).

Some qualitative information on the mean orientation of the vinyls relative to the heme plane is also suggested by the present NMR NOE data. In sperm whale metMbH_2O, significant NOEs were detected between the heme methyl and the vinyl H_β peak on each of pyrroles I and II (Unger et al., 1985). Such NOEs can be expected for cis-oriented vinyl groups which are not too far out of plane (dihedral angles $\leq 30°$). However, in *Aplysia* metMb, we are unable to detect any NOE between the 3-CH_3 (peak C) and the 4-vinyl H_β (peak U). This suggests that the vinyl orientation for at least the 4-vinyl group is more out-of-plane or at least exhibits more oscillatory mobility in *Aplysia* metMb than in sperm whale metMb. Preliminary analysis of the vinyl orientations in crystals of *Aplysia* metMb are consistent with this picture (M. Bolognesi, unpublished results).

Conclusions

We have shown by using *Aplysia limacina* metMb as a test case that simple NMR spectroscopy techniques can be used to describe important aspects of the molecular and electronic structure of the heme cavity in a ferric heme protein. Thus, specific deuterium labeling of the heme has provided the spectral assignment of several heme side chains in the acidic form of the protein and has enabled us to recognize the presence of heme rotational disorder to an extent larger than observed in mammalian Mbs. In the high-spin acidic form of the protein, in spite of the fast relaxation rates, the nuclear Overhauser effect was successfully applied to confirm the spectral assignments, locate and distinguish protons belonging to a heme methylene pair, and derive the orientation of propionate and vinyl side chains. In this same acidic form of *Aplysia* Mb, the sixth binding site is known to be empty. We found that the chemical shift of the heme *meso* resonances is a diagnostic and sensitive probe for the coordination of a water molecule to the heme: the *meso* protons are located upfield (−20 ppm), as compared to their position in the spectrum of sperm whale metMbH_2O (+40 ppm). Furthermore, the temperature dependence of the chemical shifts of the *meso* resonances displays a deviation from the Curie behavior that is consistent with a thermally accessible Kramers doublet with significant $S = {}^3/_2$ character. On the other hand, the temperature dependence of propionate and vinyl chemical shifts shows selective deviation which can be interpreted in terms of thermally induced side-chain reorientation.

All the above methods, which have led us to a qualitative description of the heme pocket in *Aplysia limacina* metMb, are of general applicability and will allow comparison with other heme proteins.

Registry No. Heme, 14875-96-8.

References

Antonini, E., & Brunori, M. (1971) *Hemoglobin and Myoglobin in Their Reaction with Ligands*, North-Holland, Amsterdam.

Ascoli, F., Rossi Fanelli, M. R., & Antonini, E. (1981) *Methods Enzymol. 76*, 72–87.

Bolognesi, M., Coda, A., Batti, G., Ascenzi, P., & Brunori, M. (1985) *J. Mol. Biol. 183*, 113–115.

Brunori, M., Antonini, E., Fasella, P., Wyman, J., & Rossi Fanelli, A. (1968) *J. Mol. Biol. 34*, 497–504.
Budd, D. L., La Mar, G. N., Langry, K. C., Smith, K. M., & Nayyir-Mazhir, R. (1979) *J. Am. Chem. Soc. 101*, 6091–6096.
Carrington, A., & McLachlan, A. D. (1967) *Introduction to Magnetic Resonance*, Chapter 12, Harper, New York.
Davis, N. L. (1982) Ph.D. Thesis, University of California.
Giacometti, G. M., Das Ros, A., Antonini, E., & Brunori, M. (1975) *Biochemistry 14*, 1584–1588.
Giacometti, G. M., Ascenzi, P., Brunori, M., Rigatti, S., Giacometti, G., & Bolognesi, M. (1981) *J. Mol. Biol. 151*, 315–319.
Goff, H., & Shimomura, E. (1980) *J. Am. Chem. Soc. 102*, 31–37.
Iizuka, T., & Morishima, I. (1975) *Biochim. Biophys. Acta 400*, 143–153.
Ilgenfritz, G., & Schuster, T. M. (1971) in *Probes of Structure and Function of Macromolecules and Membranes*, Vol. 2, pp 299–310, Academic, New York.
Jesson, J. P. (1973) in *NMR of Paramagnetic Molecules* (La Mar, G. N., Horrocks, W. D., Jr., & Holm, R. H., Eds.) pp 1–51, Academic, New York.
Jue, T., Krishnamoorthi, R., & La Mar, G. N. (1983) *J. Am. Chem. Soc. 105*, 5701–5702.
La Mar, G. N. (1973) in *NMR of Paramagnetic Molecules* (La Mar, G. N., Horrocks, W. D., Jr., & Holm, R. H., Eds.) pp 85–126, Academic, New York.
La Mar, G. N. (1979) in *Biological Applications of Magnetic Resonance* (Shulman, R. G., Ed.) pp 305–343, Academic, New York.
La Mar, G. N., & Walker-Jensen, F. A. (1978) in *The Porphyrins* (Dolphin, D., Ed.) Vol. IV, pp 61–157, Academic, New York.
La Mar, G. N., Budd, D. L., Viscio, D. B., Smith, K. M., & Langry, K. C. (1978) *Proc. Natl. Acad. Sci. U.S.A. 75*, 5755–5759.
La Mar, G. N., Budd, D. L., Smith, K. M., & Langry, K. C. (1980a) *J. Am. Chem. Soc. 102*, 1822–1827.
La Mar, G. N., Smith, K. M., Gersonde, K., Sick, H., & Overkamp, M. (1980b) *J. Biol. Chem. 255*, 66–70.
La Mar, G. N., Jackson, J. T., & Bartsch, R. G. (1981) *J. Am. Chem. Soc. 103*, 4405–4410.
La Mar, G. N., Krishnamoorthi, R., Smith, K. M., Gersonde, K., & Sick, H. (1983a) *Biochemistry 22*, 6239–6246.
La Mar, G. N., Davis, N. L., Parish, D. W., & Smith, K. M. (1983b) *J. Mol. Biol. 168*, 887–896.
Lecomte, J. T. J., Johnson, R. D., & La Mar, G. N. (1985) *Biochim. Biophys. Acta 829*, 268–274.
Leigh, J. S., Maltempo, M., Ohlsson, P., & Paul, K. (1975) *FEBS Lett. 51*, 304–308.
Maltempo, M. M., Moss, T. H., & Cusanovich, M. A. (1974) *Biochim. Biophys. Acta 342*, 290–305.
McGrath, T. M., & La Mar, G. N. (1978) *Biochim. Biophys. Acta 539*, 99–111.
Morishima, I., Shiro, Y., & Wakino, T. (1985) *J. Am. Chem. Soc. 107*, 1063–1065.
Noggle, J. H., & Shirmer, R. E. (1971) *The Nuclear Overhauser Effect*, Academic, New York.
Parish, D. W. (1984) Ph.D. Dissertation, University of California.
Reed, C. A., Mashiko, T., Bentley, S. P., Kastner, M. E., Scheidt, W. R., Spartalian, K., & Lang, G. (1979) *J. Am. Chem. Soc. 101*, 2948–2958.
Rossi Fanelli, A., & Antonini, E. (1957) *Biokhimiya (Moscow) 22*, 335–344.
Rossi Fanelli, A., & Antonini, E. (1960) *J. Biol. Chem. 235*, P5.
Rotilio, G., Calabrese, L., Giacometti, G. M., & Brunori, M. (1971) *Biochim. Biophys. Acta 236*, 234–237.
Satterlee, J. D. (1986) *Annu. Rep. NMR Spectrosc. 17*, 79–178.
Smith, K. M., & Pandey, R.K. (1983) *J. Heterocycl. Chem. 20*, 1383–1388.
Smith, K. M., Eivazi, F., Langry, K. C., Baptista de Almeida, J. A. P., & Kenner, G. W. (1979) *Bioorg. Chem. 8*, 485–495.
Smith, K. M., Parish, D. W., & Inouye, W. S. (1986) *J. Org. Chem. 51*, 666–671.
Steigemann, W., & Weber, E. (1979) *J. Mol. Biol. 127*, 309–338.
Takano, T. (1977) *J. Mol. Biol. 110*, 537–568.
Tentori, L., Vivaldi, G., Carta, S., Marinucci, M., Massa, M., Antonini, E., & Brunori, M. (1971) *FEBS Lett. 12*, 181–186.
Unger, S. W., Lecomte, J. T. J., & La Mar, G. N. (1985) *J. Magn. Reson. 64*, 521–526.
Wittenberg, B. A., Brunori, M., Antonini, E., Wittenberg, J. B., & Wyman, J. (1965) *Arch. Biochem. Biophys. 111*, 576–579.